

## Transient oscillations and dynamic Stark effect in semiconductors

M. Lindberg and S. W. Koch

*Optical Sciences Center and Physics Department, University of Arizona, Tucson, Arizona 85721*

(Received 20 October 1987)

Oscillatory structures in the differential probe transmission spectra of semiconductors are calculated assuming pump-probe excitation with very short pulses. For the case of resonant interband excitation the oscillations occur around the central pump frequency. They evolve into the spectral hole with increasing temporal overlap between pump and probe pulses. Under nonresonant excitation conditions, oscillatory structures around the exciton resonance are computed. These oscillations occur as precursors of the optical Stark shift.

### I. INTRODUCTION

Coherent light-matter interaction has been extensively studied in the framework of quantum optics and two-level-atom spectroscopy,<sup>1</sup> where the characteristic dephasing times are long in comparison to available laser pulses. In a semiconductor the absorbed light generates electron-hole excitations which experience a variety of scattering processes leading to a very rapid relaxation of the originally coherent coupling between exciting light and medium polarization. Therefore one has to use very short optical pulses to study coherent processes in semiconductors.<sup>2</sup> Anisotropic state filling in Ge,<sup>3</sup> phase coherence and orientational relaxation of excitons in GaAs,<sup>4</sup> as well as coherent coupling effects in pump-probe spectroscopy<sup>5,6</sup> have been investigated using picosecond pulses. In the femtosecond time domain, the optical Stark shift,<sup>7,8</sup> spectral hole burning,<sup>9-12</sup> and oscillatory structures in differential transmission spectra<sup>13</sup> have been observed.

In this paper we present the theoretical analysis of the femtosecond experiments reported in Ref. 13, where the strong pump pulse excites the medium polarization, which is measured by a weak, spectrally broad probe pulse. We extend our earlier work<sup>14</sup> to discuss also transmission changes around the exciton resonance for two different excitation conditions and we study the effects of damping. We concentrate on two characteristic situations, in which (i) the pump pulse resonantly excites the interband transitions in the semiconductor and the probe measures the transmission changes in the vicinity of the pump frequency, or (ii) in which the pump pulse is detuned from the exciton resonance but the probe measures the changes right at the exciton resonance. In any case, we concentrate on the very early times after the excitation, when different  $k$  states can be assumed to react independently to the exciting light. We compute transmission spectra which can be compared to the results of ultrafast pump-probe experiments, where the changes of the pulse envelopes are so rapid that their spectral characteristics become important. In our theory the dipole-coupled  $k$  states of the valence and conduction bands are modeled as inhomogeneously broadened transitions. The  $k$ -mixing many-body Coulomb effects are ig-

nored, Coulomb attraction is kept, and the most important aspect of the scattering processes among the elementary excitations is included as decay of the electron or hole out of the dipole-coupled spectral region. Clearly, this simple picture has to be revised as soon as the many-body effects become dominant.<sup>15</sup>

After deriving an expression for the semiconductor transmission spectrum (Sec. II), we analyze in Sec. III oscillatory structures in the differential transmission with emphasis on the influence of carrier and polarization relaxation processes. In Sec. IV we study transient transmission changes at the exciton resonance and we discuss the relation of the transmission oscillations to the optical Stark shift of the exciton. After summarizing our results in Sec. V, we analyze in the Appendix the modifications which are expected for larger temporal widths of the probe pulse.

### II. DIFFERENTIAL TRANSMISSION SPECTRA

As in the femtosecond experiments,<sup>13</sup> we investigate the situation of a semiconductor which is illuminated by mutually coherent pump and probe pulses traveling in a small angle relative to each other. For this case we showed in Ref. 14 that the equation for the slowly varying amplitude of the probe pulse can be written in the form

$$\frac{\partial}{\partial x} \mathcal{E}_p + \frac{1}{c} \frac{\partial}{\partial t} \mathcal{E}_p = \frac{i\Omega}{2\epsilon_0 c} \mathcal{P}_p. \quad (1)$$

Here,  $x$  is the propagation direction,  $\Omega$  is the rapid oscillation frequency, and  $\mathcal{P}_p$  is the amplitude of that component of the induced medium polarization which oscillates in phase with the probe beam. In order to neglect the pulse deformation due to propagation, we assume that the total beam-propagation distance  $L$  is sufficiently short, i.e.,  $L \ll c \Delta t$ , where  $\Delta t$  is the temporal pulse width. This condition is well satisfied in the experiments reported in Ref. 13, allowing us to approximately solve Eq. (1) as

$$\mathcal{E}_p(x, t) = \mathcal{E}_p(0, t) + i \frac{\Omega}{2\epsilon_0 c} \int_0^x dy \mathcal{P}_p(y, t). \quad (2)$$

As usual, we define the optical susceptibility  $\chi$  as the linear response of the medium to the weak probe field. In the spatially homogeneous case we have

$$\mathcal{P}_p(x, t) = \int_{-\infty}^t dt' \chi(t, t') \mathcal{E}_p(x, t'). \quad (3)$$

The response function  $\chi$  may be separated into two parts,

$$\chi(t, t') = \chi_0(t - t') + \delta\chi(t, t'), \quad (4)$$

where  $\chi_0(t - t')$  is the background contribution which has its origin in the unperturbed material properties and  $\delta\chi(t, t')$  represents the perturbation caused by the pump pulse. This perturbation is not a function of the time difference because the pump pulse breaks the temporal translation invariance. In the experiments,<sup>13</sup> one mea-

sures the differential transmission  $\delta T(\omega)$ , which can be expressed as

$$\delta T(\omega) = \frac{|\mathcal{E}_p(L, \omega)|_{\text{pump on}}^2 - |\mathcal{E}_p(L, \omega)|_{\text{pump off}}^2}{|\mathcal{E}_p(L, \omega)|_{\text{pump off}}^2}, \quad (5)$$

where

$$\mathcal{E}_p(L, \omega) = \int_{-\infty}^{\infty} dt e^{i(\omega - \Omega_L)t} \mathcal{E}_p(L, t)$$

is the Fourier transform of the probe field after traveling through the sample and  $\Omega_L$  is the central frequency of the pump pulse. Assuming that the linear susceptibility is only weakly structured in the frequency region of interest, we obtain, from Eqs. (3) and (5),

$$\delta T(\omega) = -\frac{L\Omega}{2\pi\epsilon_0 c |\mathcal{E}_p(0, \omega)|^2} \text{Im} \left[ \mathcal{E}_p^*(0, \omega) \int_{-\infty}^{\infty} d\omega' \mathcal{E}_p(0, \omega') \int_{-\infty}^{\infty} dt e^{i(\omega - \omega')t} \int_0^{\infty} dt' e^{i(\omega - \Omega_L)t'} \delta\chi(t + t', t) \right] + O(|\delta\chi|^2). \quad (6)$$

Equation (6) can be simplified if the temporal width of the probe pulse is negligibly small in comparison to that of the pump pulse. For such a temporally short probe pulse with a correspondingly broad spectral distribution, one can write the approximate relation

$$\mathcal{E}_p(0, \omega') \mathcal{E}_p^*(0, \omega) \cong |\mathcal{E}_p(0, \omega)|^2 e^{-i(\omega - \omega')t_p}. \quad (7)$$

Inserting (7) into Eq. (6) yields

$$\delta T(\omega) \propto -\text{Im} \left[ \int_0^{\infty} dt e^{i(\omega - \Omega_L)t} \delta\chi(t + t_p, t_p) \right]. \quad (8)$$

Here and in the following we take the peak of the pump pulse as origin of time,  $t = 0$ , and denote by  $t_p$  the delay of the probe pulse. Negative values of  $t_p$  indicate that the probe reaches the sample before the peak of the pump, i.e., during the rising part of the pump pulse. We study the effects of a finite temporal width of the probe pulse in the Appendix of this paper, where we show that for most situations of experimental relevance it is acceptable to neglect the probe width justifying the use of Eq. (8) instead of (6). For mathematical convenience, we use an exponential shape for the pump pulse in the form

$$\mathcal{E}_L(t) = e_L e^{-\sigma|t|}. \quad (9)$$

In the time regime such pulses have a discontinuity in their derivative, but in the frequency regime they are smoothly varying functions simulating physical pulses rather well. Moreover, in our expressions for the differential transmission spectra, we always have to integrate over the pulse amplitudes. Due to these integrations the discontinuity in the pulse slope does not influence the results considerably.

### III. RELAXATION EFFECTS

The semiconductor is modeled as discussed in Ref. 14, but additionally we include also damping of the polarization and populations. As mentioned in the Introduction, we analyze the two situations where (i) the excitation occurs well into the band and the probe detects the spectral region of the pump pulse, or (ii) where the central pump frequency is well below the exciton and the probe-transmission changes occur around the exciton resonance. To discuss the spectral regime of the exciton resonance, the contributions of the band states may be neglected in a very simple approximation and the system may be described by a single transition. On the other hand, when the interband transitions are discussed, we have to deal with a continuum of  $k$  states and, consequently, we have to sum over all individual contributions.

In case (i) each  $k$  state is described<sup>16</sup> by the following coupled set of differential equations:

$$\frac{\partial}{\partial t} n_e = i\mu[\mathbf{E}(t)p - \mathbf{E}^*(t)p^*] - \Gamma n_e, \quad (10a)$$

$$\frac{\partial}{\partial t} n_h = i\mu[\mathbf{E}^*(t)p^* - \mathbf{E}(t)p] - \Gamma n_h, \quad (10b)$$

$$\frac{\partial}{\partial t} p^* = -[ie(k) + \gamma]p^* - i\mu\mathbf{E}(t)(1 - n_e - n_h). \quad (10c)$$

Here,  $n_e$  ( $n_h$ ) is the number of electrons (holes) at state  $k$ ,  $p^*$  is the polarization of the state  $k$ , and  $\mu$  is the dipole matrix element. The only explicit  $k$  dependence is in the transition energy  $e(k)$ . The field  $\mathbf{E}$  has been treated in the rotating-wave approximation,

$$\mathbf{E}(t) = \mathcal{E}_L(t) e^{i(\mathbf{k}_L \cdot \mathbf{r} - \Omega_L t)} + \mathcal{E}_p(t) e^{i(\mathbf{k}_p \cdot \mathbf{r} - \Omega_L t)}. \quad (11)$$

Because the probe field is broad banded, the central frequency is taken to be the laser frequency for sake of convenience.

To motivate our treatment of the decay processes, we assume that the  $k$  space can be divided into two parts: a resonant part containing the  $k$  states which interact directly with the laser field and the remaining nonresonant part. Equations (10a)–(10c) are only used to describe the resonant states. For these states the decay rate  $\Gamma$  simulates the intraband scattering out of the resonantly coupled part into the nonresonant part. The validity of Eqs. (10a)–(10c) for band-to-band transitions is restricted to short times, i.e., to the fast transient regime where electron and hole populations are still small. At later times Coulomb effects like band-edge reduction and phase-space filling become increasingly important, even-

tually changing the dynamics of the system.

In case (ii) we can still use Eqs. (10a)–(10c) where  $k$  now labels the exciton state,<sup>16</sup> and  $\Gamma$  is the decay rate of the exciton due to radiative or nonradiative recombination. This decay is usually considerably slower than the intraband relaxation of the carriers.

Using an iterative integration procedure, we solve Eqs. (10a)–(10c) in third order in the field amplitude  $\mathbf{E}(t)$ . The initial values of the system are taken as the steady-state values without field. The induced polarization is given as

$$\mathbf{P} = \mu(p + p^*) . \quad (12)$$

Using Eqs. (3), (4), and (12) we can extract the differential susceptibility  $\delta\chi$  in the form

$$\begin{aligned} \delta\chi(t, t') = & -2i\mu^4 \left[ e^{-[i(e-\Omega_L)+\gamma](t-t')} \left\{ \int_0^\infty dt'' e^{-\Gamma t''} \mathcal{E}_L(t'-t'') \int_0^\infty dt''' e^{[i(e-\Omega_L)-\gamma]t'''} \mathcal{E}_L^*(t'-t''-t''') \right. \right. \\ & \left. \left. + \int_0^\infty dt'' e^{-\Gamma t''} \mathcal{E}_L^*(t'-t'') \int_0^\infty dt''' e^{-[i(e-\Omega_L)+\gamma]t'''} \mathcal{E}_L(t'-t''-t''') \right\} \right. \\ & + e^{-\Gamma(t-t')} \int_0^{t-t'} dt'' e^{-[i(e-\Omega_L)+\gamma-\Gamma]t''} \mathcal{E}_L(t-t'') \int_0^\infty dt''' e^{[i(e-\Omega_L)-\gamma]t'''} \mathcal{E}_L^*(t'-t''') \\ & \left. + e^{-[i(e-\Omega_L)+\gamma](t-t')} \int_0^{t-t'} dt'' \mathcal{E}_L(t-t'') \int_0^{t-t'-t''} dt''' e^{-\Gamma t'''} \mathcal{E}_L^*(t-t''-t''') e^{[i(e-\Omega_L)+\gamma]t'''} \right] . \quad (13) \end{aligned}$$

To analyze the influence of relaxation effects, we discuss in the remainder of this section the case of resonant interband excitation well above the semiconductor band gap. In this case we have to sum Eq. (13) over the whole  $k$  space. As a consequence of the electron-hole Coulomb attraction, the density of states has to be multiplied by the Coulomb enhancement factor,<sup>16</sup> leading to a more or less structureless combined density of states, which we treat as a constant  $D$ . Consequently, the contributions of the second and fourth term of Eq. (13) vanish. Inserting the resulting expression into Eq. (8), we obtain the differential transmission as

$$\begin{aligned} \delta T(\omega) = & \frac{2L\Omega}{\epsilon_0 c} \mu^4 D \operatorname{Re} \left[ \int_0^\infty dt e^{i(\omega-\Omega_L)t} \left\{ e^{-2\gamma t} \int_0^\infty dt' e^{-\Gamma t'} \mathcal{E}_L(t_p-t') \mathcal{E}_L^*(t_p-t'-t) \right. \right. \\ & \left. \left. + e^{-\Gamma t} \int_0^t dt' e^{-(2\gamma-\Gamma)t'} \mathcal{E}_L(t+t_p-t') \mathcal{E}_L^*(t_p-t') \right\} \right] . \quad (14) \end{aligned}$$

This formula is rather general, but still we can deduce some results straightforwardly from it. Neglecting all relaxation mechanisms, we showed in Ref. 14 that spectral transmission oscillations occur which are centered around the central frequency of the pump pulse. These results are exactly reproduced if we set  $\gamma$  and  $\Gamma$  to zero in Eq. (14). Examples for the coherent oscillations are plotted in Fig. 1 for different values of  $t_p$ . Figure 1 shows that the period of the oscillations is inversely proportional to the time delay between probe and pump. For zero delay, Fig 1(c), only one underswing is left besides the central peak. For positive  $t_p$  (not shown) this underswing also vanishes and the oscillatory structures evolve into the spectral hole.

To investigate the influence and relative importance of the different damping mechanisms, we now consider the case of an extremely short dipole damping time  $1/\gamma$ . After partial integration and letting  $\gamma \rightarrow \infty$ , Eq. (14) yields

$$\delta T(\omega) \propto \frac{2\gamma}{(\omega-\Omega_L)^2 + (2\gamma)^2} \int_0^\infty dt e^{-\Gamma t} |\mathcal{E}_L(t_p-t)|^2 - \operatorname{Re} \left[ \frac{1}{2\gamma - i(\omega-\Omega_L)} \mathcal{E}_L^*(t_p) \int_0^\infty dt e^{[i(\omega-\Omega_L)-\Gamma]t} \mathcal{E}_L(t+t_p) \right] . \quad (15)$$

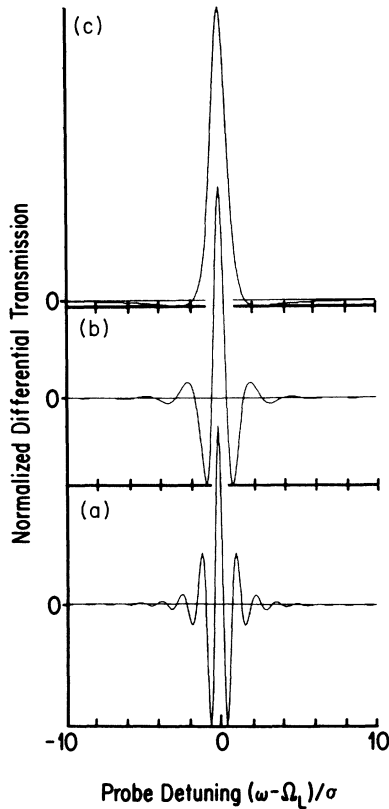


FIG. 1. Normalized differential transmission spectra calculated for the case of interband excitation. The central pump frequency  $\Omega_L$  is assumed to be well above the semiconductor band gap. The temporal width (FWHM) of the pump pulse, Eq. (9), is 120 fs and all damping processes have been ignored. Panels (a)–(c) show the spectra for different time delays  $t_p$  between pump and probe, where the probe precedes the pump maximum: (a)  $t_p = -400$  fs, (b)  $t_p = -200$  fs, and (c)  $t_p = 0$ .

The first term depends only on the pump-field values before the arrival of the probe pulse. This term has a Lorentzian structure describing the saturation of the transition by the already-generated population. The second term on the right-hand side (rhs) of (15) depends on the pump-field values at times equal to or later than  $t_p$ . This term is always oscillatory in frequency if the integrand has a peak in the range of integration. Such a peak is possible for negative  $t_p$ , i.e., for the probe pulse preceding the pump. A numerical evaluation shows that we obtain oscillations similar to those shown in Fig. 1 even for very large dipole damping. Only the overall magnitude of the transmission spectra decreases with increasing  $\gamma$ .

The influence of the population relaxation rate is much more delicate. Using the exponential pulse shape (9), we integrate Eq. (14) to obtain the differential transmission for negative  $t_p$  as

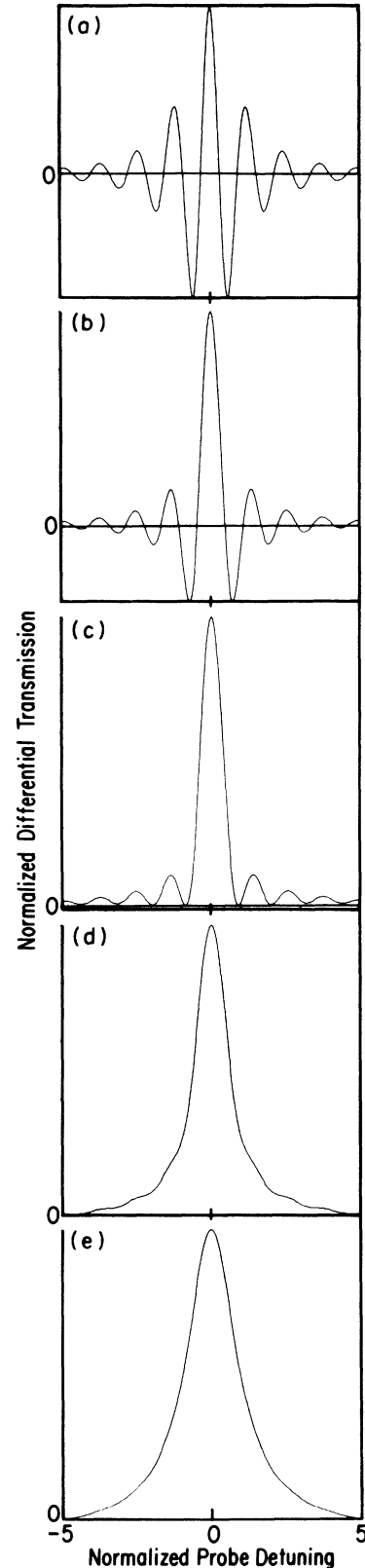


FIG. 2. Normalized differential transmission spectra for interband excitation. The spectra are plotted vs detuning,  $(\omega - \Omega_L)/\sigma$ , from the central pump frequency  $\Omega_L$  for a fixed time delay  $t_p = -5/\sigma$ . The dipole damping  $\gamma$  has been kept constant as  $2.51\sigma$  and the ratio of population damping and width of the pump pulse, Eq. (9), has been varied: (a)  $\Gamma/\sigma = 0$ ; (b)  $\Gamma/\sigma = 0.8$ ; (c)  $\Gamma/\sigma = 1.2$ ; (d)  $\Gamma/\sigma = 1.6$ ; (e)  $\Gamma/\sigma = 2.0$ .

$$\delta T(\omega) = C |e_L|^2 \text{Re} \left[ \frac{e^{\sigma t_p}}{(\sigma + 2\gamma - i\Delta)(\sigma - \Gamma + i\Delta)} \left( \frac{2\sigma}{\sigma + \Gamma - i\Delta} e^{-(i\Delta - \Gamma)t_p} - \frac{\sigma + 2\Gamma - i\Delta}{\Gamma + 2\sigma} e^{\sigma t_p} \right) \right]. \quad (16)$$

The detuning  $\omega - \Omega_L$  is denoted  $\Delta$ . Again, we can see that increasing the dipole damping  $\gamma$  only decreases the magnitude of the spectrum but the structure remains essentially unchanged.

In Fig. 2 we show differential transmission spectra for various values of  $\Gamma/\sigma$  for the case of  $t_p = -5/\sigma$ . The dipole damping  $\gamma$  is kept constant with the value  $\gamma = 2.51\sigma$ . We see that increasing  $\Gamma/\sigma$  causes a decrease in the amplitude of the oscillatory features and the central peak becomes more and more dominant. For large values of  $\Gamma/\sigma$ , the oscillations disappear completely, and only a Lorentzian spectrum remains. The critical value for  $\Gamma/\sigma$  is approximately 1. We can loosely say that if the decay of the population is faster than the change of the pump amplitude, the pump pulse appears for the semiconductor almost like a continuous wave for which

oscillatory patterns are not expected.

Increasing the value of  $\Gamma/\sigma$  can be done experimentally by changing the temporal width [fullwidth at half maximum (FWHM)],  $\Delta t \cong (2 \ln 2)/\sigma$ , of the pump pulse. Since  $\Gamma$  is fixed for a particular sample and fixed excitation conditions, varying the pulse width allows to measure the sequence of patterns shown in Fig. 2. Hence, this scenario can be used in femtosecond pump-probe experiments to measure the population damping rate  $\Gamma$  by monitoring the vanishing of the coherent oscillations by increasing the temporal pulse width for fixed probe-pump delay.

Assuming a population decay rate  $\Gamma = 1/100 \text{ fs}^{-1}$ , we show in Fig. 3 the oscillatory structures around the central pump frequency for otherwise the same conditions as in Fig. 1. A comparison between Figs. 1 and 3 reveals that the most prominent consequences of the dissipative processes are the reduction of the oscillation amplitudes with respect to the central peak and the pronounced broadening of the central peak with increasing temporal overlap between probe and pump.

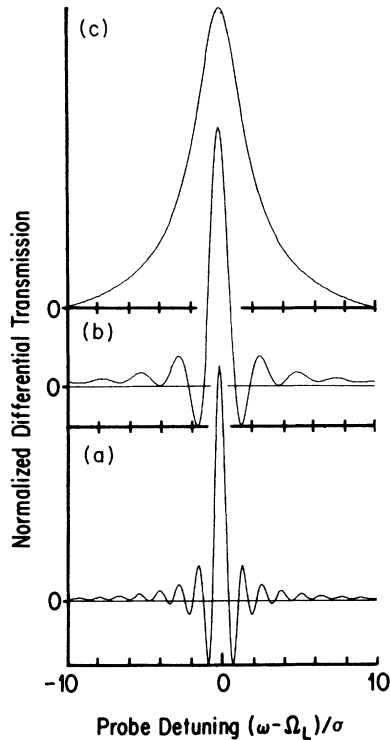


FIG. 3. Normalized differential transmission spectra calculated for interband excitation. The central pump frequency  $\Omega_L$  is assumed to be well above the semiconductor band gap. The temporal FWHM of the pump pulse, Eq. (9), is 120 fs and the damping constants have been taken as  $\gamma = 0.035 \text{ fs}^{-1}$  and  $\Gamma = 1/100 \text{ fs}^{-1}$ . (a)–(c) are for different time delays  $t_p$  between pump and probe, where the probe precedes the pump maximum: (a)  $t_p = -400 \text{ fs}$ , (b)  $t_p = -200 \text{ fs}$ , and (c)  $t_p = 0$ .

#### IV. NONRESONANT EXCITATION OF THE EXCITON

To study the coherent structures in the spectral vicinity of the exciton resonance, we assume that the exciton relaxation time is relatively long in comparison to that of the band states. This assumption seems to be quite reasonable because the exciton does not suffer the rapid intraband scattering which is most responsible for the coherence decay of interband transitions at very early times. Since we ignore effects like phase-space filling and Coulomb screening, we can describe the exciton transition as a dipole-coupled two-level transition.<sup>16</sup> In this case Eqs. (10a)–(10c) can be applied and the result in Eq. (13) is valid when the number of the  $k$  states is reduced into one.

In the following we concentrate on the case of a pump pulse which is spectrally detuned from the exciton resonance. Actually, this allows both nonresonant excitation spectrally below the exciton as well as interband excitation. Even though our treatment is best applicable for the case of excitation in the transparent region of the crystal, we may still use it also as a simple approximation for the case of interband excitation since the contributions of the band states and of the exciton are simply additive.<sup>16</sup>

Inserting (13) into (8) and assuming for convenience  $\Gamma = 2\nu$  and  $\gamma = \nu$  and that the pulse duration is much shorter than  $\nu^{-1}$ , we obtain the differential transmission in the form

$$\delta T(\omega) \propto 2\mu^4 \left[ \frac{2\nu}{\nu^2 + \Delta^2} \operatorname{Re} \left[ \int_{-\infty}^{t_p} dt \int_{-\infty}^t dt' \mathcal{E}_L(t) \mathcal{E}_L^*(t') e^{i(e - \Omega_L)(t-t')} \right] + \operatorname{Re} \left[ \frac{1}{\nu - i\Delta} \int_0^\infty dt \mathcal{E}_L(t + t_p) e^{[i(\omega - \Omega_L) - 2\nu]t} \int_{-\infty}^{t+t_p} dt' \mathcal{E}_L^*(t') e^{[i(e - \Omega_L) - \nu](t_p - t')} \right] \right]. \quad (17)$$

Here,  $\Delta = \omega - e$  is the probe detuning from the exciton resonance and  $\nu$  is the exciton linewidth. The oscillatory structures of  $\delta T$  are contained in the second term on the rhs of Eq. (17); the first integral is independent of  $\omega$ . However, because of the prefactor  $1/(\nu - i\Delta)$  the oscillations now occur around  $\Delta = 0$ , i.e., around the exciton resonance  $e$  and not around the laser frequency  $\Omega_L$ .

Using the exponential pulse shape, Eq. (9), we analytically evaluate Eq. (17). Since the lengthy mathematical expressions allow no more physical insight than Eq. (17) itself, we present only the resulting spectra. Assuming nonresonant excitation spectrally below the exciton resonance, we plot in Fig. 4 the differential transmission spectra for fixed pump frequency and varying delay time. For negative  $t_p$  we see oscillatory structures around the exciton resonance. These oscillations are not symmetric as in the case of the interband transitions because the pump laser is detuned with respect to the exciton resonance.

When the delay time approaches zero, the oscillatory structures disappear, leaving a differential transmission which has an almost dispersive shape. This dispersive shape indicates that the exciton resonance has been shifted to higher energies (increased transmission on the low-energy side and decreased transmission on the high-energy side). This is the so-called light shift (dynamic Stark shift), which has recently been observed for the 1s exciton in semiconductors.<sup>7,8</sup> Hence, we see that the coherent oscillations evolve continuously into the dynamic Stark shift.

To study the amplitude decrease of the oscillatory structures with increasing detuning from the resonance, we evaluate Eq. (17) for the case of large detunings. If the detuning exceeds both the exciton linewidth and the spectral width of the pump pulse, we can write the asymptotic behavior of  $\delta T$  as

$$\delta T(\omega) = \frac{L\Omega}{\pi\epsilon_0 c} \mu^4 \frac{1}{e - \Omega_L} \operatorname{Im} \left[ -\frac{1}{\nu - i\Delta} \int_0^\infty dt |\mathcal{E}_L(t + t_p)|^2 e^{i(\Delta - \nu)t} \right] + O((e - \Omega_L)^{-2}). \quad (18)$$

This equation shows that the amplitude falls off inversely proportional to the detuning of the pump, but the shape of the spectral structures is detuning independent, allowing the observation of oscillatory structures around the exciton resonance even for large detunings. Note that for cw excitation, i.e.,  $\mathcal{E}_L(t) = \text{const}$ , Eq. (18) becomes

$$\delta T(\omega) = -\frac{L\Omega}{\pi\epsilon_0 c} \mu^4 \frac{|\mathcal{E}_L|^2}{e - \Omega_L} \frac{2\nu\Delta}{(\nu^2 + \Delta^2)^2}, \quad (19)$$

which clearly exhibits a dispersive shape similar to the result obtained for a simple frequency shift of an absorption line. The proportionality of the transmission changes to  $|\mathcal{E}_L|^2$  and the inverse proportionality to the laser detuning are the characteristic signatures of the Stark shift.

## V. CONCLUSIONS

In conclusion, we have studied oscillatory structures in the differential transmission spectra of semiconductors. As shown in Ref. 13, our results agree well with the experimental findings. We analyzed the effect of population and polarization damping using a simple model for the

decay mechanisms. For the situation when the transmission changes are observed around the pump pulse, the physical origin of the oscillatory structures may be described as a transient population grating created by the pump and probe pulses together. This grating is generated during the time of overlap between the pulses and the oscillations in the spectra are manifestations of the total interference between the probe pulse and that part of pump pulse which is scattered from the grating into the direction of the probe beam. This explanation is valid when the phase-coherence time is very short and the fields are weak. Strong fields have been discussed in Ref. 14 and they were shown to bring new effects.

To obtain a better understanding of the oscillatory transmission changes, it is instructive to discuss the situation when the pump-induced changes are small in comparison to the total transmitted probe field.<sup>13</sup> In this case one can write

$$E_p(L, \omega) |_{\text{pump on}} = E_p(L, \omega) |_{\text{pump off}} + \delta E_p(L, \omega) |_{\text{pump on}}. \quad (20)$$

Inserting (20) into (5) and ignoring quadratic terms in  $\delta E_p$  yields

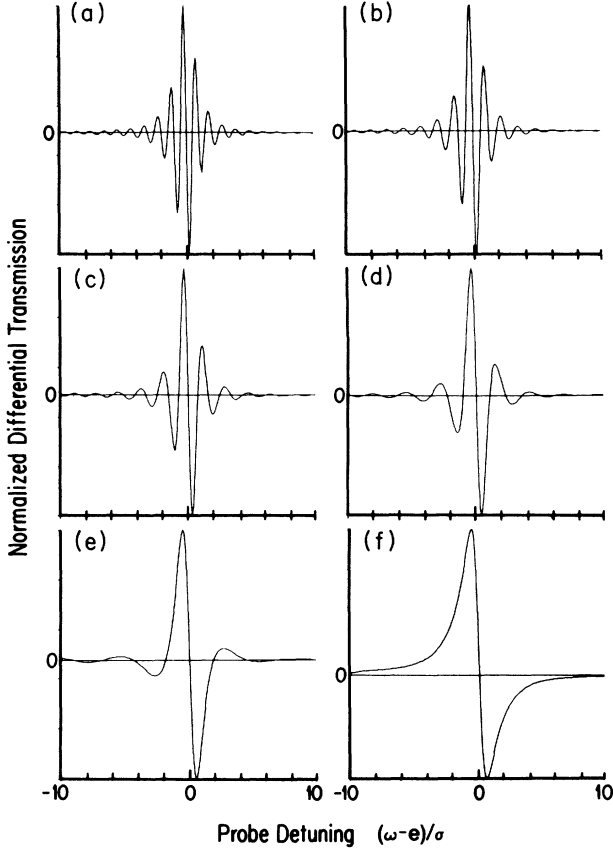


FIG. 4. Normalized differential transmission spectra in the spectral vicinity of the exciton resonance  $e$ . The central pump frequency  $\Omega_L$  is assumed to be detuned  $-10\sigma$ , where  $\sigma^{-1} = 120/(2 \ln 2)$  fs, and the temporal width (FWHM) of the pump pulse, Eq. (9), is 120 fs. (a)–(f) are for different time delays  $t_p$  between pump and probe, where the probe precedes the pump maximum: (a)  $t_p = -500$  fs, (b)  $t_p = -400$  fs, (c)  $t_p = -300$  fs, (d)  $t_p = -200$  fs, (e)  $t_p = -100$  fs, and (f)  $t_p = 0$ .

$$\delta T(\omega) \cong \frac{2 \operatorname{Re}[E_p^*(L, \omega) |_{\text{pump off}} \delta E_p(L, \omega) |_{\text{pump on}}]}{|E_p(L, \omega) |_{\text{pump off}}|^2}, \quad (21)$$

showing, that the differential transmission spectra can be viewed as measuring the interference between the unperturbed transmitted probe field and the pump-induced change in the transmitted probe field.

Our analysis of the different decay mechanisms indicates that the dipole relaxation in our model is quite unimportant since it influences the spectra only by changing their overall magnitude. However, the oscillatory structures are rather sensitive to population damping. We have also presented a simple theory for the non-resonant excitation spectrally below the exciton resonance. Oscillatory structures have been computed which evolve into the optical Stark shift for increasing temporal overlap between pump and probe pulses.

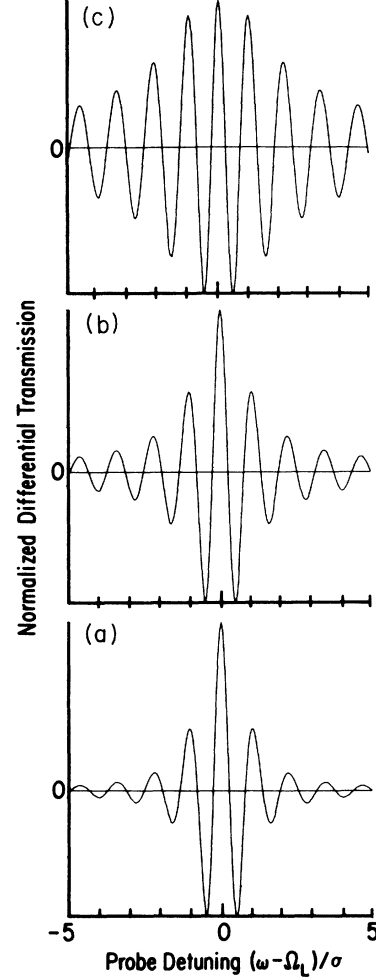


FIG. 5. Normalized differential transmission spectra for different temporal widths of the probe pulse, Eq. (A4). The time delay has been kept constant as  $t_p = -5.1/\sigma$ ,  $\sigma^{-1} = 120/(2 \ln 2)$  fs, damping has been neglected, and the probe-pulse parameter  $\eta$  has been varied: (a)  $\eta^{-1} = 40$  fs, (b)  $\eta^{-1} = 80$  fs, and (c)  $\eta^{-1} = 160$  fs.

## ACKNOWLEDGMENTS

We want to thank N. Peyghambarian, Optical Sciences Center, University of Arizona, for many discussions on femtosecond experiments. Our work is financially supported through the Optical Circuitry Cooperative, University of Arizona. A grant for computer time at the John von Neuman Computer Center, Princeton University, is gratefully acknowledged.

## APPENDIX

In this Appendix we discuss the effects caused by a finite temporal width of the probe pulse. If the probe pulse amplitude is real and symmetric around the time  $t_p$ , the differential transmission, Eq. (6), can be written in the form

$$\delta T(\omega) \propto -\frac{1}{|\mathcal{E}_p(0, \omega)|} \text{Im} \left[ \int_{-\infty}^{\infty} dt \mathcal{E}_p(0, t) e^{i(\omega - \Omega_L)(t - t_p)} \int_0^{\infty} dt' e^{i(\omega - \Omega_L)t'} \delta\chi(t + t', t) \right]. \quad (\text{A1})$$

A rough estimate indicates that the inner integral in Eq. (A1) changes as a function of the parameter  $t$  on the same time scale as the pump pulse. Hence, if the probe pulse is shorter than the pump pulse, or, equivalently, if its frequency spectrum is much broader than that of the pump pulse, the  $\delta$ -function approximation should be good. However, to obtain quantitative results on the importance of the finite probe-pulse width, we need an explicit expression for the change in the susceptibility.

We start from Eq. (13), but to keep the situation as simple as possible, we now ignore all relaxation effects. As an example, we choose the situation of band-to-band transitions. In this case, after setting  $\gamma$  and  $\Gamma$  equal to

zero in (13) and summing over the  $k$  states, the expression for the differential susceptibility takes the form

$$\delta\chi(t, t') \cong -i2\mu^4 D(e_{\text{res}}) \int_0^{\infty} dt'' \mathcal{E}_L(t - t'') \mathcal{E}_L^*(t' - t''). \quad (\text{A2})$$

Again, the joint density of states is taken as constant. Explicit results are obtained using the pump-pulse shape of Eq. (9) and the probe-pulse shape

$$\mathcal{E}_p(t) = e_p e^{-\eta|t - t_p|}. \quad (\text{A3})$$

Evaluating Eq. (A1) yields

$$\delta T(\omega) \propto \frac{\Delta^2 + \eta^2}{\eta} \text{Re} \left[ \left[ \frac{\eta e^{2\sigma t_p}}{\sigma(\sigma + i\Delta)[(2\sigma + i\Delta)^2 - \eta^2]} - \frac{4\sigma\eta e^{(-i\Delta + \sigma)t_p}}{(\sigma^2 + \Delta^2)(\sigma - i\Delta)(\sigma^2 - \eta^2)} \right] + e^{(-i\Delta + \eta)t_p} \left[ \frac{2\sigma - i\Delta}{\sigma(\sigma - i\Delta)^2(\eta - i\Delta)} - \frac{1}{2\sigma(\sigma - i\Delta)(2\sigma + \eta - i\Delta)} - \frac{1}{2\sigma(\sigma + i\Delta)(2\sigma - \eta + i\Delta)} + \frac{2\sigma}{(\sigma^2 + \Delta^2)(\sigma - i\Delta)(\sigma - \eta)} \right] \right], \quad (\text{A4})$$

when  $t_p$  is negative. As illustrative examples we plot in Fig. 5 some spectra where we fixed the spectral width  $\sigma$  of the pump pulse and varied the width  $\eta$  of the probe pulse. For  $\eta > \sigma$  the spectra are essentially unchanged in comparison to those obtained by approximating the probe pulse as a  $\delta$  function in time. Significant deviations are obtained only when the spectral width of the probe pulse becomes smaller than that of the pump pulse.

<sup>1</sup>L. Allen and J. H. Eberly, *Optical Resonances and Two-Level Atoms* (Wiley, New York, 1975).

<sup>2</sup>See, e.g., the articles in *Ultrashort Light Pulses*, Vol. 18 of *Topics in Applied Physics*, edited by S. L. Shapiro (Springer-Verlag, Berlin, 1977); in *High Excitation and Short Pulse Phenomena*, edited by M. H. Pilkuhn [J. Lumin. **30** (1984)]; J. Opt. Soc. Am. B **2**, 474 (1986).

<sup>3</sup>A. L. Smirl, T. F. Boggess, B. S. Wherrett, G. P. Perryman, and A. Miller, Phys. Rev. Lett. **49**, 933 (1982).

<sup>4</sup>L. Schultheis, J. Kugl, and A. Honold, Phys. Rev. Lett. **57**, 1797 (1986).

<sup>5</sup>A. Von Jena and H. E. Lessing, Appl. Phys. **19**, 131 (1979).

<sup>6</sup>S. L. Palfrey and T. F. Heinz, J. Opt. Soc. Am. B **2**, 674 (1985).

<sup>7</sup>A. Mysyrowicz, D. Hulin, A. Antonetti, A. Migus, W. T. Masselink, and H. Morkoç, Phys. Rev. Lett. **56**, 2748 (1986).

<sup>8</sup>A. Von Lehmen, D. S. Chemla, J. E. Zucker, and J. P. Heritage, Opt. Lett. **11**, 609 (1986).

<sup>9</sup>J. L. Oudar, A. Migus, D. Hulin, G. Grillon, J. Etchepare, and A. Antonetti, Phys. Rev. Lett. **55**, 2074 (1985).

<sup>10</sup>W. H. Knox, R. L. Fork, M. C. Downer, D. A. B. Miller, D. S. Chemla, C. V. Shank, A. Gossard, and W. Wiegmann, Phys. Rev. Lett. **56**, 1191 (1986).

<sup>11</sup>N. Peyghambarian and S. W. Koch, Rev. Phys. Appl. **22**, 1711 (1987).

<sup>12</sup>W. Z. Lin, R. W. Schönlein, S. D. Brorson, J. G. Fujimoto, and E. P. Ippen, paper TUJJ2, Proceedings of the International Quantum Electronics Conference IQEC '87, Baltimore, 1987 (unpublished); E. Ippen, in Proceedings of the U.S.-Japan Conference, Monterey, 1987 (unpublished).

<sup>13</sup>B. Fluegel, N. Peyghambarian, G. Olbright, M. Lindberg, S. W. Koch, M. Joffre, D. Hulin, A. Migus, and A. Antonetti, Phys. Rev. Lett. **59**, 2588 (1987); M. Joffre, D. Hulin, A. Migus, A. Antonetti, C. Benoit à la Guillaume, N. Peyghambarian, M. Lindberg, and S. W. Koch, Opt. Lett. **13**, 276 (1988).

<sup>14</sup>M. Lindberg and S. W. Koch, J. Opt. Soc. Am. B **5**, 139 (1988).

<sup>15</sup>See, e.g., the articles in *Optical Nonlinearities and Instabilities in Semiconductors*, edited by H. Haug (Academic, New York, 1988); H. Haug and S. Schmitt-Rink, Prog. Quantum Electron. **9**, 3 (1984); L. Banyai and S. W. Koch, Z. Phys. B **63**, 283 (1986).

<sup>16</sup>M. Lindberg and S. W. Koch, Phys. Rev. B **38**, 3342 (1988).